Cement and Concrete Research 167 (2023) 107117

Contents lists available at ScienceDirect

Cement and Concrete Research

journal homepage: www.elsevier.com/locate/cemconres

Toward performance improvement of supersulfated cement by nano silica: Asynchronous regulation on the hydration kinetics of silicate and aluminate

Heng Chen [a], Pengkun Hou [a,b,*], Xiangming Zhou [b], Leon Black [c], Samuel Adu-Amankwah [c], Pan Feng [d], Na Cui [e], Michał A. Glinicki [f], Yamei Cai [g], Shipeng Zhang [g], Piqi Zhao [a,**], Qinfei Li [a,**], Xin Cheng [a,**]

[a] Shandong Provincial Key Lab for the Preparation & Measurement of Building Materials, University of Jinan, Jinan, Shandong 250022, China
[b] Department of Civil & Environmental Engineering, Brunel University London, Uxbridge, Middlesex UB8 3PH, UK
[c] School of Civil Engineering, University of Leeds, Woodhouse Lane, LS29JT, UK
[d] School of Materials Science and Engineering, Southeast University, Nanjing, Jiangsu 211189, China
[e] School of Civil Engineering and Architecture, University of Jinan, Jinan, Shandong 250022, China
[f] Institute of Fundamental Technological Research, Polish Academy of Sciences, Pawinskiego 5b, 02-106 Warsaw, Poland
[g] Department of Civil and Environmental Engineering, The Hong Kong Polytechnic University, Hong Kong

ARTICLE INFO

Keywords:
Supersulfated cement
Nano silica
Gypsum content
Mechanical property
Microstructure

ABSTRACT

Supersulfated cement (SSC) is a traditional low-carbon cement, but its slow hydration and strength development has limited its practical applications. Nano silica (NS) was used to activate the hydration of SSC by taking advantage of its ability to regulate silicate and aluminate reactions. The mechanical performance of various mixes was determined, as a function of sulfation degree and NS addition, as pore structure, phase assemblage, hydration degree, and microstructure. Results showed that NS improves the hydration degree of slag, densifies the microstructure, and significantly increases both early- and late-age compressive strength. The enhancement was attributed to its effects on the hydration of slag in SSC: delaying ettringite formation, but promoting C-(A)-S-H precipitation, reducing microporosity. This study reveals the critical role of the regulation of hydration kinetics of silicate and aluminate in controlling the performance of SSC as NS does.

1. Introduction

CO_2 emissions associated with Portland cement production is a major sustainability challenge to the cement industry. Low-carbon alternatives, such as calcium sulfoaluminate cement (CSA) [1] and supersulfated cement (SSC) [2], have been developed to partially replace Portland cement with the aim of reducing the CO_2 emissions of the cement industry. As a classic low-carbon cement, SSC, has attracted attention recently, thanks to its ultra-low clinker content, utilization of solid wastes, and excellent sulfate resistance [3–5]. Similar to CSA, the main hydration products of SSC are ettringite (AFt) and aluminum incorporated calcium silicate hydrates (C-(A)-S-H) [6]. Unlike CSA, practical application of SSC is limited due to its lower early strength.

The low early-age strength of SSCs is attributed to the slow dissolution rate of slag [7,8]. Early-age strength can be improved by increasing the amount of Portland cement, but this can decrease the long-term compressive strength of hardened SSC mortars [1,9]. This phenomenon has not been resolved completely, and possible reasons could be the inhibition of slag dissolution by the preferred precipitation of AFt [9] or hydrotalcite [10] on the surface of slag in SSC with high alkali content in the presence of excess Portland cement. On top of this, it has also been found that the addition of alkalis, such as KOH or NaOH, or alkali sulfate cannot increase the strength of SSC [9,11], although Briki et al. showed that slag has much higher reactivity in NaOH solution than in cement paste [12]. There seems to exist an optimal pH range for the hydration of SSC, especially for the precipitation of AFt [1,2]. Recently, sodium lactate had been found to increase the compressive strength of SSC [3,11] and it was proposed that the chelation of lactate on the surface of slag could promote the breaking of silicon-oxygen network [3].

* Correspondence to: P. Hou, Shandong Provincial Key Lab for the Preparation & Measurement of Building Materials, University of Jinan, Jinan, Shandong 250022, China.
** Corresponding authors.
E-mail addresses: pkhou@163.com (P. Hou), mse_zhaopq@ujn.edu.cn (P. Zhao), mse_liqf@ujn.edu.cn (Q. Li), chengxin@ujn.edu.cn (X. Cheng).

https://doi.org/10.1016/j.cemconres.2023.107117
Received 6 August 2022; Received in revised form 2 February 2023; Accepted 5 February 2023
Available online 10 February 2023

Table 1
Chemical compositions of Portland cement and GGBS in this study.

	CaO	SiO_2	Al_2O_3	SO_3	Fe_2O_3	MgO	LOI[a]	SSA (m^2/kg)
Portland cement	64.39	21.88	4.31	2.56	3.47	1.72	1.42	340
GGBS	30.20	32.78	17.55	2.30	1.45	6.36	9.36	531

[a] Lost on ignition.

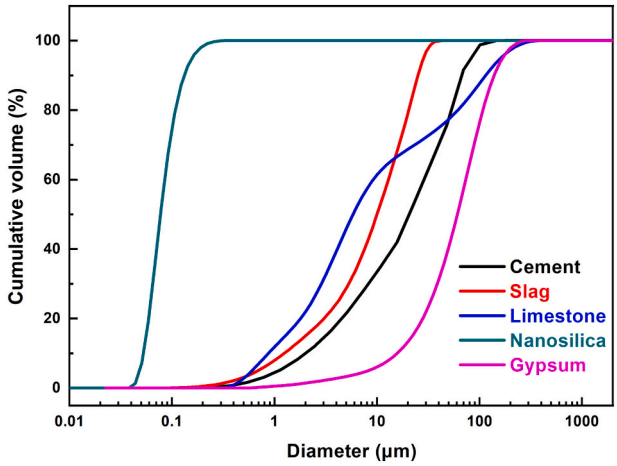

Fig. 1. The particle size distribution of the raw materials in this study.

From above, most of the published literature on SSC appears to focus on methods for promoting the dissolution of slag, in order to accelerate the hydration of SSC. However, from the principle of chemical equilibrium, both the dissolution of reactants and the precipitation of reaction products are frequently coupled with each other and both of them are responsible for the reaction rate [8], as in the Portland cement system [13,14]. Therefore, accelerating the precipitation of hydration products could be another way to promote the hydration process. It has long been found that the addition of nucleation seeds would increase the early strength of cementitious materials, such as calcium silicate hydrate (C-S-H) seeds in Portland cement systems [15], and AFt seeds in SAC system [16]. Similar to C-S-H seeds, nano silica (NS) exhibits the capacity of providing nucleation sites for C-S-H and accelerate the hydration kinetics of Portland cement at early age [17,18]. Since C-(A)-S-H is one of the two main hydration products of SSC [2], the addition of nano silica could accelerate the hydration of SSC. In fact, Ma et al. [19] found the addition of 3 wt% of NS increased the compressive strength of SAC at 8 h, 1 day, and 56 days by ~42 %, ~38 %, and ~65 %, respectively through promoting hydration of SAC and densifying its microstructure. Since SSC shares similar hydration products with SAC, the addition of NS could enhance the hydration of SSC. Li et al. [20] found 1 wt% of NS increased the compressive strength of CSA/Portland cement at 2 h and 28 days by ~42 % and ~20 %, respectively. In addition, Hou et al. [21] proposed that NS has a contrary influence on the precipitation of AFt and C-(A)-S-H in the system of $CaSO_4$-C_3S-C_3A. Thus, NS could modify the ratio of the two main hydration products (C-(A)-S-H and AFt) which could further affect the hydration and performance of SSC.

Therefore, to reveal the effect of NS on SSC hydration and performance, SSC was prepared with either 4 or 10 % gypsum and with part of the slag replaced by NS (3 wt% of total mass). It is shown that NS significantly promotes the hydration kinetics, densifies the microstructure, and increases the mechanical strength of SSC. The role of NS in the regulation of aluminate and silicate precipitation is also discussed.

2. Materials and methods

2.1. Materials

The main components of SSC are ground granulated blast furnace slag (Luxinxincai Co., Ltd. Shandong, China), cement (China United Cement Linyi Co., Ltd. Shandong, China) and gypsum (Shanghai Macklin Biochemical Technology Co., Ltd., Shanghai, China). The chemical and mineral compositions of the slag and Portland cement (Chinese P·I 42.5) are presented in Table 1. It can be noted that it is an acid slag, indicating its low reactivity. Gypsum used was of analytical grade. The NS had a diameter of 7–40 nm, and a specific surface area of 380 m^2/g. The particle size distributions of slag, Portland cement and gypsum are shown in Fig. 1. The naphthalene superplasticizer from Sobute was used for preparing cement pastes and mortars. Chinese standard sand was used in the mortars. In addition, limestone powder with particle size <150 μm, was added in SSC, considering its stabilization effect on AFt and synergetic effect with aluminosilicate [22,23].

2.2. Preparation of samples

The preparing of the samples is based on the Chinese standard 'GB/T 17671-2021'. The formulations of the mixes investigated in this study are shown in Table 2. In the four mixes, the clinker and limestone content were kept the same, and the GGBS content varied with the gypsum and NS content, since the amount of GGBS is always abundant. The water to binder (Cement + GGBS + Gypsum + Limestone + NS) ratio (w/b) of all the paste samples was 0.4 and that of all the mortar samples was 0.5 for ensuring the flowability while avoiding bleeding. NS was first ultrasonically dispersed in tap water for 30 min with a 1.08 kW ultrasonic cell crusher. For the samples with NS, plasticizer was added to obtain similar fluidity to the samples without NS. The limestone was considered a mineral admixture, and as such its content was maintained at 10 %.

After specified durations of standard curing (RH > 95 %, 20 ± 2 °C), paste samples were hydration stopped by immersion in pure isopropanol initially for 24 h and then in fresh isopropanol for a further 7 days, after which they were dried in a vacuum oven at 40 °C for 3 days. The dried hardened pastes were then placed in a vacuum desiccator before characterization by mercury intrusion porosimetry (MIP), X-ray diffraction

Table 2
Mixture proportion in this study.

Samples	Clinker	GGBS	Gypsum	Limestone	NS	Superplasticizer	
						Paste	Mortar
G4	5	81	4	10	–	–	–
G4N3	5	78	4	10	3	1.5	2.5
G10	5	75	10	10	–	–	–
G10N3	5	72	10	10	3	1.5	2.5

'G' is for the percentage of gypsum in the SSC, 'N' is for the percentage of NS.

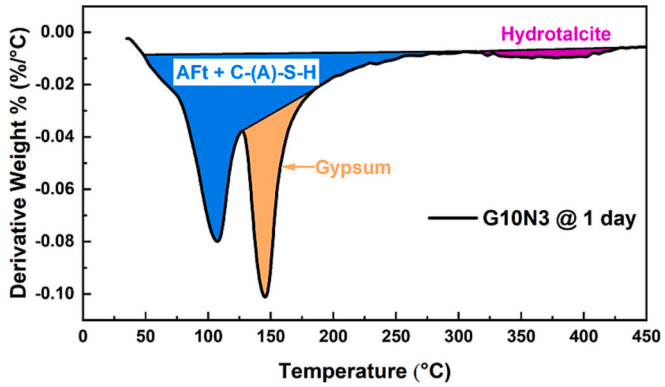

Fig. 2. Schematic diagram of quantifying the bound water content of different phases by TG.

(XRD), thermal gravity (TG), scanning electron microscopy (SEM).

2.3. Methods

2.3.1. Compressive and flexural strength of hardened SSC mortars

In accordance with the Chinese standard 'GB/T 17671-2021', prismatic mortar specimens of 4 cm × 4 cm × 16 cm were made and their compressive and flexural strength were measured at 1, 3, 7, 28, 56, and 90 days.

2.3.2. Porosity of hardened SSC pastes

The porosity of hardened SSC pastes was measured at 90 days by MIP (Micromertics, AutoPore IV 9500). Around 2-3 g of dried paste pieces were used for each test. The contact angle was set to 130°. The equilibration time during the intrusion of mercury was 10 s. The applied pressure ranged from 0.5 to 55,000 psi, corresponding to ~355 um to ~3.3 nm, according to the Washburn's Equation.

2.3.3. Characterization of hydration products of the SSC pastes

2.3.3.1. Quantitative analysis of hydration products. The quantities of the principal hydration products were estimated using bound water contents, derived from thermal gravimetry. Around 20–30 mg of hydration stopped powdered paste was used for the TGA test, and the mass change recorded over the temperature range 30–1000 °C, at a heating rate of 10 °C/min, in an argon atmosphere (flow rate: 50 ml/min). The mass loss over the range 50–530 °C has been attributed to the bound water within C-(A)-S-H, AFt, gypsum, AFm, and hydrotalcite [3,7,24], since there is no portlandite in the system [8]. Furthermore, the 'tangential method' was used to determine each hydration product following Scrivener et al. [24]. The bound water peak of gypsum is around 140 °C [25]. The bound water content from the residual gypsum (BW_{Gyp}), can be estimated as in Fig. 2.

Thus, the residual gypsum (M_{Gyp}) can be calculated based on its bound water content (BW_{Gyp}), and the percentage of bound water in gypsum (ω_{Gyp} around 20.9 %) by the following formula:

$$M_{Gyp} = BW_{Gyp}/\omega_{Gyp} \quad (1)$$

The mass loss over the range 300–500 °C was attributed to the bound water of hydrotalcite [3,7,24]. The mass of hydrotalcite (M_{Ht}) formed upon hydration can be estimated based on its bound water content (BW_{Ht}, which is determined as in Fig. 2.) and the percentage of bound water in hydrotalcite (ω_{Ht} around 45 % [24,26]) by the following formula:

$$M_{Ht} = BW_{Ht}/\omega_{Ht} \quad (2)$$

Bound water in both C-(A)-S-H and AFt are lost at overlapping temperatures. Therefore, selective dissolution with 5 wt% Na_2CO_3 solution was used to remove the AFt and so as to determine the bound water of the C-(A)-S-H. This was performed according to [7], but with a dry mass of hardened SSC of 0.30 ± 0.01 g. The weight loss of the dried residual solid over the range 50–300 °C was considered as the bound water content of C-(A)-S-H ($BW_{C-(A)-S-H}$). Based on this, and assuming around 20 % bound water in C-(A)-S-H ($\omega_{C-(A)-S-H}$) [24,26], the mass of C-(A)-S-H produced ($M_{C-(A)-S-H}$) can be estimated by the following formula:

$$M_{C-(A)-S-H} = BW_{C-(A)-S-H}/\omega_{C-(A)-S-H} \quad (3)$$

Combining the total weight loss over the range 50–300 °C, the bound water content of AFt (BW_{AFt}), gypsum (BW_{Gyp}), the percentage of bound water in AFt (ω_{AFt}, around 45.9 % [24,26]), the mass of AFt (M_{AFt}) produced can be calculated according to the following formula:

$$M_{AFt} = \left(BW_{Total} - BW_{C-(A)-S-H} - BW_{Gyp}\right)/\omega_{AFt} \quad (4)$$

Because gypsum is not a hydration product, its bound water content should be removed to determine the total bound water associated with hydration. Thus, the total chemical reaction bound water (CBW_{Total}) should be:

$$CBW_{Total} = BW_{Total} - BW_{Gyp} + BW_{Ht} \quad (5)$$

Finally, the mass of all the relevant phases (M_{Gyp}, M_{Ht}, $M_{C-(A)-S-H}$, and M_{AFt}) was normalized to the total chemical reaction bound water (CBW_{Total}).

2.3.3.2. Hydration degree of slag. Selective dissolution was used to determine the degree of slag hydration, in accordance with the Chinese standard 'GB/T 12960-2019' [27], which is similar to [7]. Using 0.15 mol/L of EDTA solution, 50 g/L of sodium hydroxide solution, and 33.3 vol% of triethanolamine (TEA) solution, 50 mL EDTA solution, 10 mL TEA solution and 120 mL distilled water was added to a 250 mL beaker. Sodium hydroxide solution was then used to adjust the pH to 11.60 ± 0.05. To this solution was added 0.30 ± 0.01 g of dry powder ground to <74 μm. The mixture was stirred using a magnetic stirrer for 30 min, after which the insoluble residue was washed with ethanol twice, with suction filtration, and dried in a vacuum oven at 105 ± 5 °C for 48 h. The degree of slag hydration (α_s) was determined by the formula:

$$\alpha_s = 1 - \frac{\frac{W_E}{1-W_{Wn}} - W_{C,0}W_{C,E}}{W_{S,0}W_{S,E}} \quad (6)$$

where: W_E: percentage of residue; W_{Wn}: chemical bound water content (CBW_{Total}); $W_{C,0}$: percentage of cement in the mixture; $W_{C,E}$: percentage of residue after the selective dissolution of pure cement; $W_{S,0}$: percentage of slag in the mixture; $W_{S,E}$: percentage of residue after the selective dissolution of slag.

2.3.3.3. Micro-morphology of the hardened pastes. The morphology of the hydration products, especially AFt, would change with hydration environment (such as the pH value of the pore solution [28]). Therefore, the morphology of the hardened pastes at 90 days was examined by SEM (Guanta FEG 250) with an acceleration voltage of 15 keV. The test samples were hydration stopped and vacuum dried as mentioned above, and their fresh surface was carbon coated before the test.

To obtain the Ca/(Si + Al) ratios of C-(A)-S-H in different systems, EDS analysis has been on polished samples with an acceleration voltage of 15 keV. For each sample, 5 different areas were tested and ten points were selected in one area. Thus, there are 50 data points of Ca/(Si + Al) ratios for one sample, from which a value with a maximum probability was obtained.

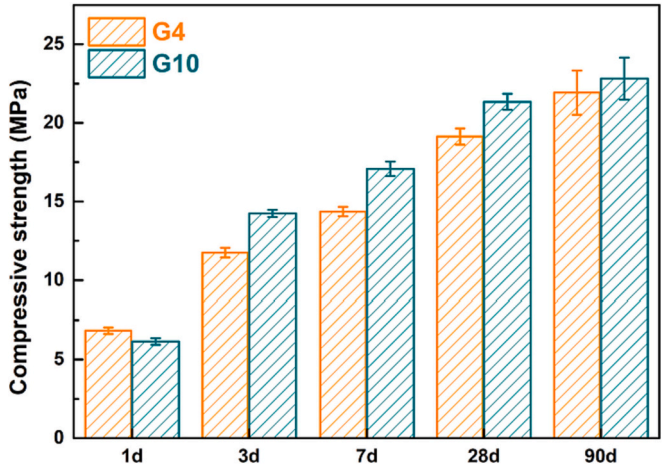

Fig. 3. Compressive strength of SSC with different gypsum content as a function of time.

3. Results

3.1. Mechanical property of hardened SSC mortars

Fig. 3 presents the compressive strength respectively of SSC with different gypsum contents. There was a gradual increase in compressive strength over time, with the samples prepared with 10 % gypsum (G10) showing slightly higher compressive strengths at all ages apart from day1. At 1 day, there remains gypsum in both systems as shown in Fig. 10a, thus G4 has higher strength due to its higher slag content. However, after 3 days, there is no gypsum in G4 as shown in Fig. 10a, therefore G4 has lower strength resulting from a lack of gypsum. However, the effect of gypsum content on compressive strength was less clear-cut, as pointed out by Luz et al. [29].

Fig. 4a and b presents the influence of NS on the compressive strength of hardened SSC mortars. Irrespective of gypsum content, the addition of NS led to a significant increase in compressive strength. While sample G4 (4% gypsum by weight) only attained a strength of ~22 MPa, even after 90 days, this doubled upon the addition of 3 % NS. The effect was slightly less pronounced for sample G10, but the addition of NS still had a significant positive impact. Fig. 4a and b also shows the compressive strength ratio between the samples prepared with and without NS. The level of positive effect of NS addition increased with curing age. The phenomenon is obviously different from the effect of NS in Portland cement system and blend cement system, in which, NS mainly improves early-age mechanical performance (i.e. the first 7 days) by filling effect and nucleation seeding effect, and pozzolanic reaction [17].

3.2. Microstructure of hardened SSC pastes

3.2.1. Porosity of hardened SSC pastes

It has been shown that the pore structure of materials is closely

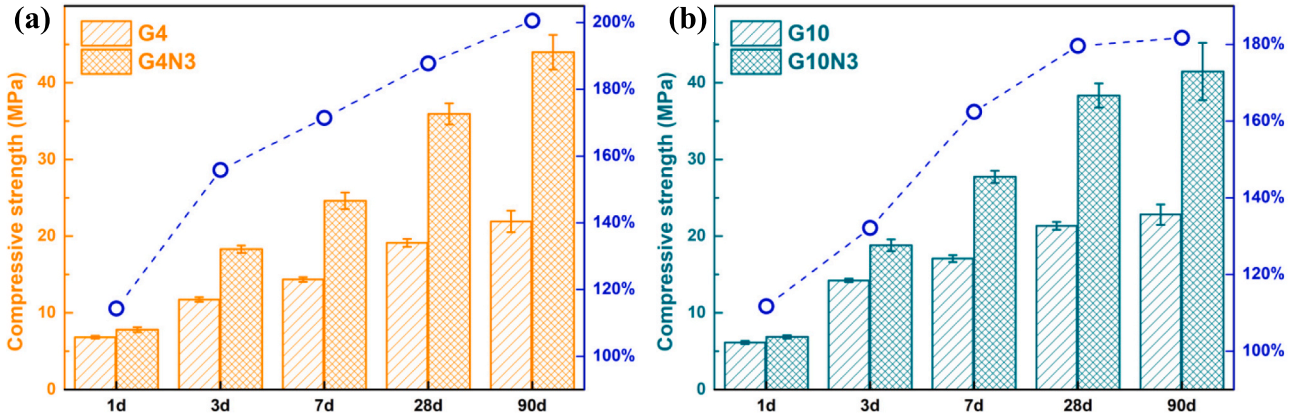

Fig. 4. Influence of NS on the compressive strength of SSC with (a) 4 % and (b) 10 % gypsum.

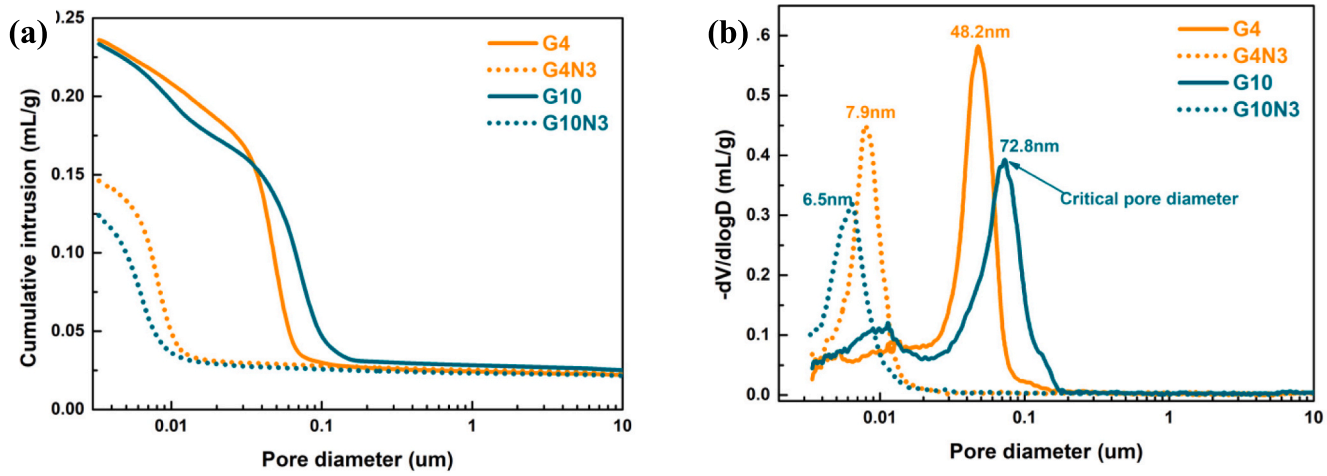

Fig. 5. (a) Porosities and (b) pore distributions of different hardened SSC pastes at 90 days.

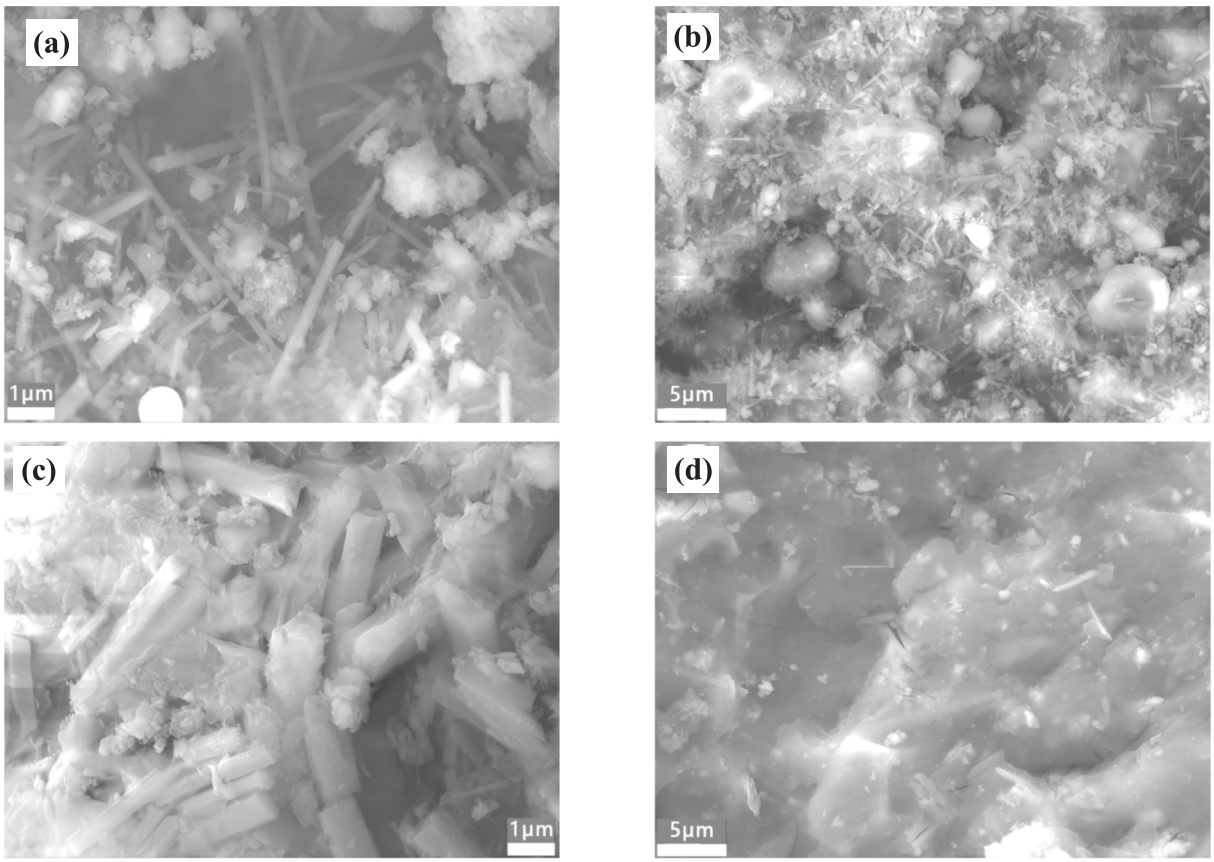

Fig. 6. Micromorphology of G4 (a: ×10,000, b: ×3000) and G4N3 (c: ×10,000, d: ×3000) at 90 days.

related to their compressive strength, with a lower porosity correlating with higher compressive strength [30]. Fig. 5a and b presents the porosities and pore distribution of the hardened SSC pastes. It can be seen from Fig. 5a that G4 and G10 has similar porosity, which is consistent with their similar compressive strength as shown in Fig. 3. However, the G4 has a smaller critical pore diameter than G10 as shown in Fig. 5b, meaning that G4 has a finer pore distribution and lower permeability.

Since NS significantly enhances SSC compressive strength (Fig. 4a and b), it is expected that these SSC systems will also show a refined pore structure.

The addition of 3 % NS decreased the cumulative mercury intrusion of the 90-day hardened samples from around 0.23 mL/g (G4 and G10) to <0.15 mL/g (G4N3 and G10N3). Taking these values, the calculated porosity of G4 and G10 was reduced from 34.1 % (G4) and 32.0 % (G10) to 20.2 % (G4N3) and 19.5 % (G10N3). Furthermore, as shown in Fig. 5b, the critical pore diameter of the hardened samples reduced significantly, from 48.2 nm (G4) and 72.8 nm (G10) to 7.9 nm (G4N3) and 6.5 nm (G10N3); equivalent to a reduction of 83.6 % and 91.0 %, respectively. The refinement of pore structure by well-dispersed NS in Portland cement-based materials has been widely reported [31–33]. This is frequently attributed to a combination of the filler effect, pozzolanic reactions, and the seeding effect [18,32,34]. However, since only traces of calcium hydroxide are formed in supersulfated cement system due to their very low Portland cement contents [9], the pozzolanic reaction is unlikely to be a significant reason for the densifying effect of NS. However, the interaction between NS and aluminate [21] could play a critical role in the hydration of slag, the main component of SSC, as elaborated in Section 3.3.

3.2.2. Morphology of hardened SSC pastes

The morphology of the hardened SSC samples prepared with 4 % gypsum is presented in Fig. 6. The overall structure of G4 is pretty porous (Fig. 6a and b), whereas that of G4N3 is much denser (Fig. 6c and d). This is consistent with the MIP data shown earlier (Fig. 5a and b). In addition, the AFt needles in G4 are thinner (approximately 0.25 μm) than those in G4N3 (approximately 1.09 μm), as shown in Fig. 8. Ma et al. [19] reported a similar effect in calcium aluminate cements, with NS leading to shorter and thicker AFt crystals. It has been found that chemical admixtures could change the morphology of AFt significantly by their absorption on the specific crystalline face or by their influence on the chemical environment of the precipitation of AFt [35]. It has been reported that the negatively-charged nano silica can be bridged by Ca ion and adsorbed on the surface of the positively-charged aluminate phase [21], which could inhibit growth of AFt and leads to shorter and thicker AFt crystals. This shorter and thicker AFt would be less expansive than the longer and thinner one [28].

The morphology of the hardened SSC samples with 10 % gypsum is presented in Fig. 7. Comparing Fig. 7a and b with Fig. 6a and b, it can be seen that gypsum content has little impact on morphology. But, Fig. 7c and d shows that the addition of NS densifies the microstructure of samples with higher gypsum contents just as for lower gypsum contents.

3.2.3. Ca/(Si + Al) of C-(A)-S-H of hardened SSC pastes

C-(A)-S-H is one of the principal hydration products, and its composition and structure play an important role in the performance of hardened pastes. It was found that the C-S-H with lower Ca/Si (from 0.7 to 2.1) has higher elastic modulus and hardness [36]. Kunther et al. [37] found that the compressive strength of C-S-H increased with the decrease of Ca/Si.

Fig. 9 presents the influence of NS on the Ca/(Si + Al) of C-(A)-S-H in the hardened pastes. It can be found that the Ca/(Si + Al) of C-(A)-S-H in the SSC system is smaller than that of Portland cement, which is consistent with the study conducted by Thomas et al. [9]. With the addition of NS, the Ca/(Si + Al) of C-(A)-S-H was reduced to around 1.0

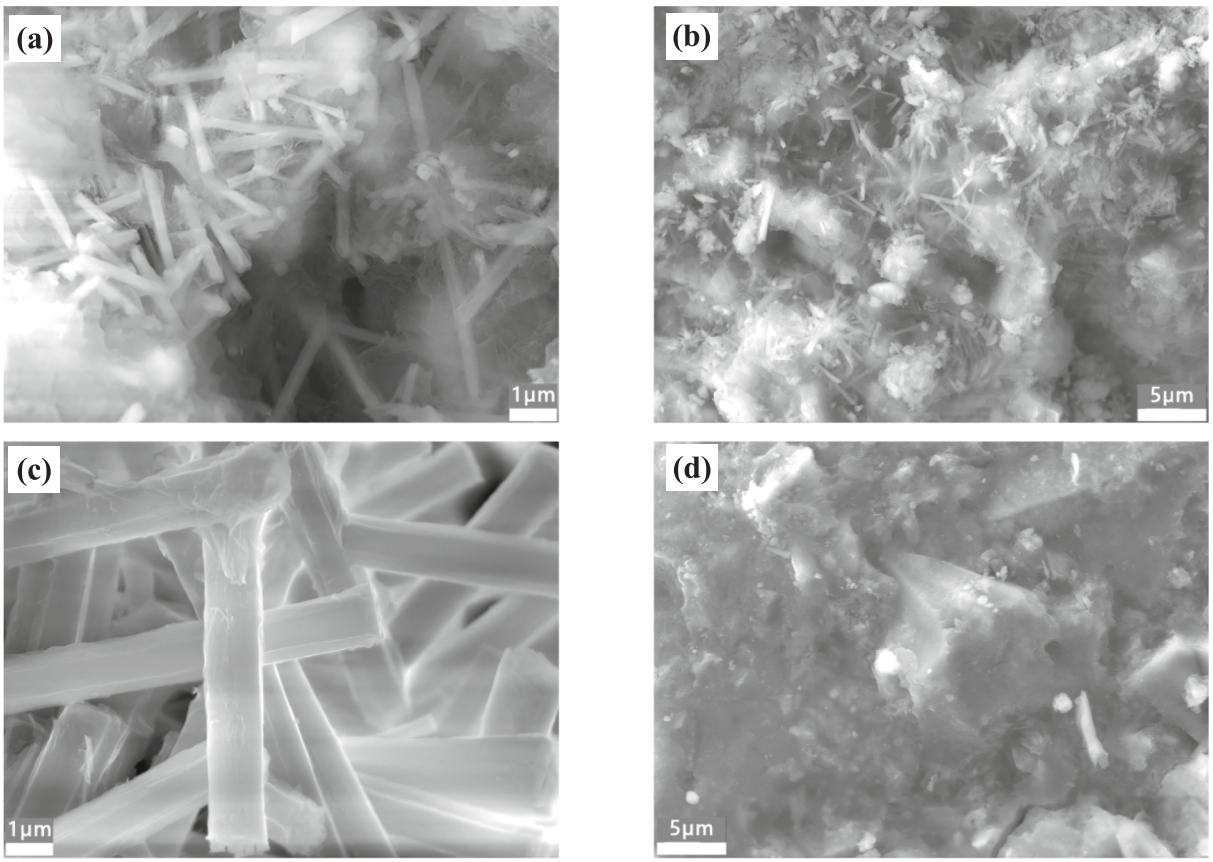

Fig. 7. Micromorphology of G10 (a: ×10,000, b: ×3000) and G10N3 (c: ×10,000, d: ×3000) at 90 days.

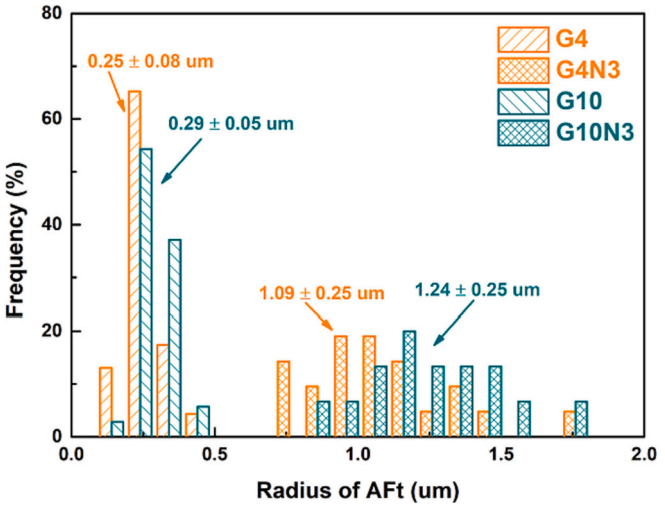

Fig. 8. Radius distribution of AFt in the samples (G4, G4N3, G10, and, G10N3) based on their SE images.

as shown in Fig. 9b, d, contributing to the higher performance of system with NS.

3.3. Phase assemblages of hardened SSC pastes

The phase assemblage of hardened pastes is a key factor dictating the SSC performance (including compressive strength). Therefore, the consumption of both gypsum and slag, plus the production of AFt and C-(A)-S-H was explored.

Fig. 10a shows the degree of gypsum consumption over time. Gypsum was almost completely consumed in sample G4 within 1 day. Meanwhile, gypsum consumption was significantly hindered by the addition of NS, with 40 % consumed by 1 day in G4N3 (2 g/100 g SSC as shown in Fig. 10b), and complete consumption only by 90 days. The same trend was seen for the samples prepared with 10 % gypsum (G10 and G10N3). The inhibiting effect of NS has been found by the authors' previous study on the C_3A + Gypsum system [21], which showed that inhibiting effect could be due to the absorption of nano silica on the surface of the positively-charged AFt.

Comparing the extent of gypsum consumption in the samples without NS (G4 and G10) (Fig. 10b) suggests that 4 % gypsum might be insufficient, since 6 g/100 g SSC was consumed within 1 day in sample G10. For the samples containing NS (G4N3 and G10N3), (Fig. 10b), gypsum consumption was faster with higher gypsum contents, indicating that the rate of gypsum consumption is related to the gypsum content.

Gypsum is consumed during the reaction with aluminates in the slag, resulting in AFt generation. This is a key factor dictating the compressive strength of hardened SSC [9]. Therefore, the amount of AFt was tracked as a function of time (Fig. 11), and there was a clear correlation between AFt contents and the consumption of gypsum, as shown in Fig. 10b. The addition of NS delayed the generation of AFt, but the final AFt content was determined by the initial gypsum content. The results also indicate that, counter to conventional understanding, the amount of AFt is not the only determinant of compressive strength in the systems with NS, since these samples develop much higher compressive strengths than those without NS.

Considering that the aluminate for AFt production is from the dissolution of slag, one would expect that the extent of slag dissolution would correlate with that of both gypsum consumption (Fig. 10b) and AFt generation (Fig. 11). However, Fig. 12, which presents the degree of

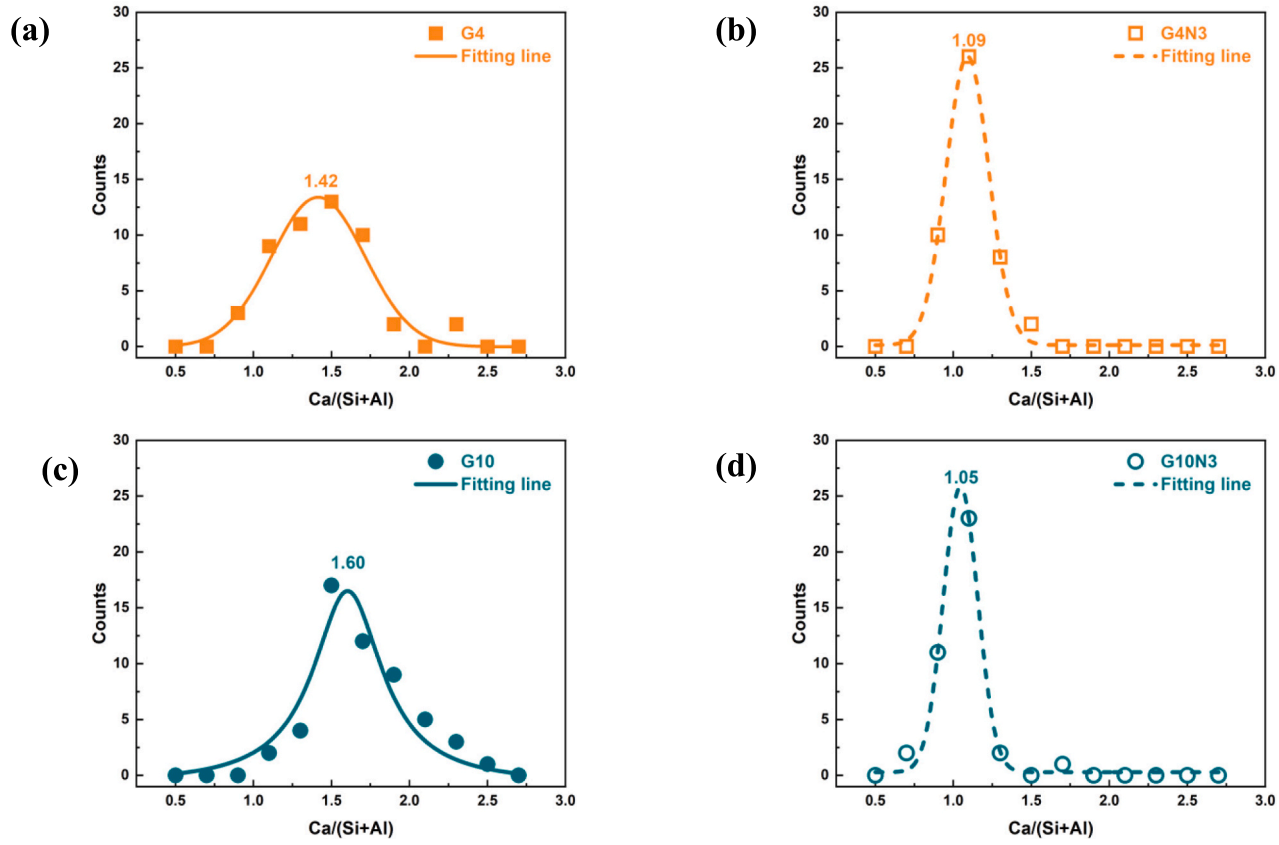

Fig. 9. Ca/(Si + Al) of C-(A)-S-H in the hardened pastes of (a) G4, (b) G4N3, (c) G10, (d) G10N3 at 90 days.

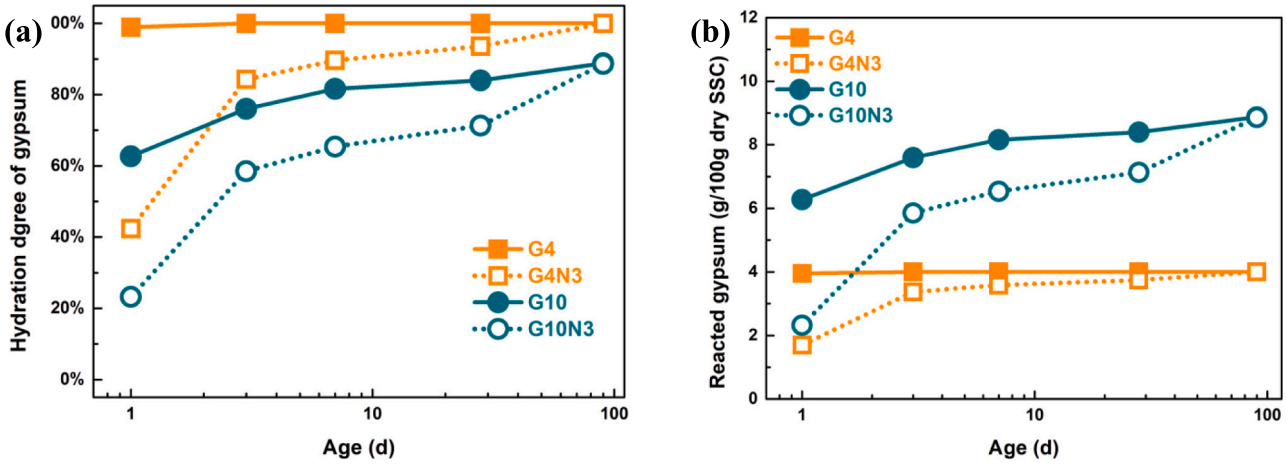

Fig. 10. (a) Hydration degree and (b) quantity of reacted gypsum as a function of time.

slag hydration as a function of time, suggests that this seems not to be the case. The degree of slag hydration in the samples with NS is much larger than that without NS after 7 days (Fig. 12), illustrating the key role of NS in promoting slag hydration. Although gypsum consumption was proportional to its content (Fig. 10b) and rate of AFt production (Fig. 11), it only slightly increases the degree of slag hydration.

There, at first, appears to be a contradiction in the role of NS; promoting the hydration of SSC (Fig. 12), yet delaying the formation of AFt (Fig. 11). What happens to the aluminate released upon slag dissolution in the presence of NS? One possible reason could be incorporation in C-(A)-S-H. The formation of C-(A)-S-H has been considered as the main reason for long-term strength enhancement [9]. Fig. 13 shows the amount of C-(A)-S-H (determined by the TG method mentioned above) formed in each system over time, highlighting the effect of NS addition. The addition of NS increases C-(A)-S-H content, particularly at later age. The formation of C-(A)-S-H provides a sink for aluminate ions released upon slag dissolution [26]. It has long been proposed that NS provides nucleation sites [18] and so promotes C-S-H formation in the Portland cement-based materials [38,39]. Here in super sulfated cement systems, NS seems to have a similar effect on the formation of C-(A)-S-H.

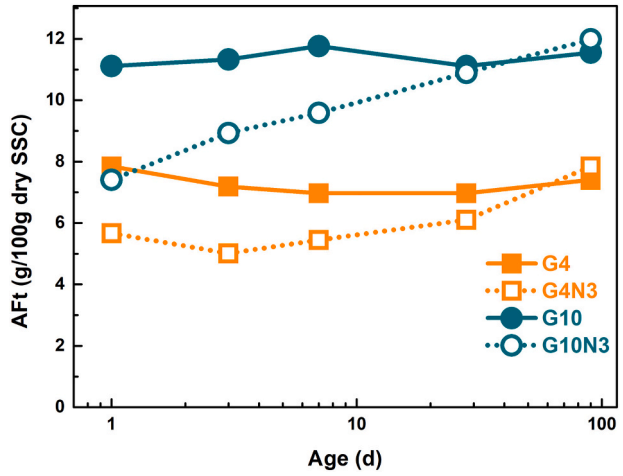

Fig. 11. Evolution of AFt as a function of time.

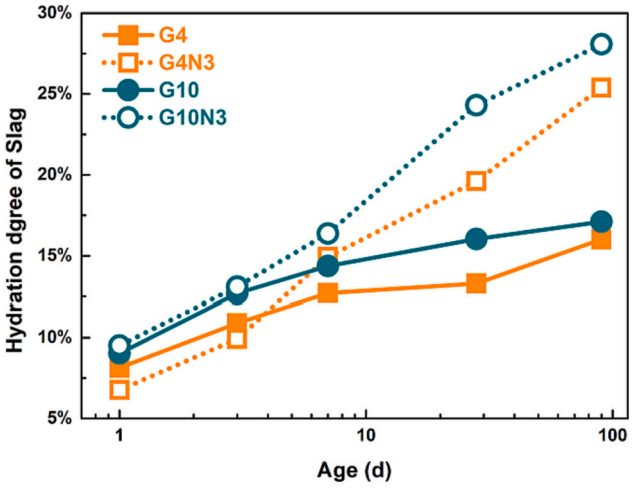

Fig. 12. Degree of slag hydration as a function of time.

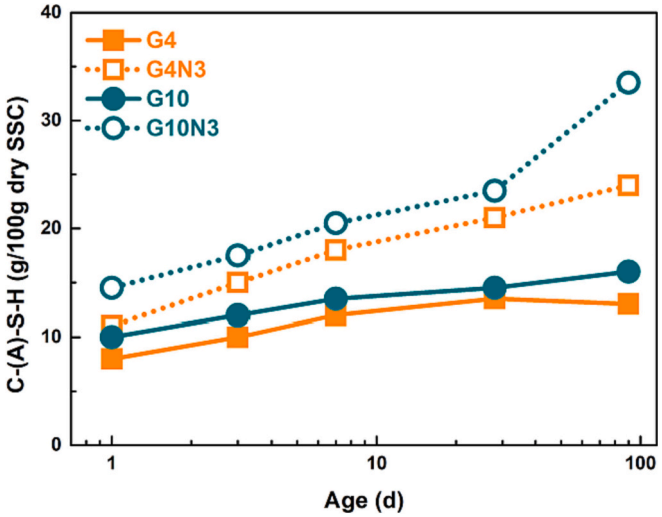

Fig. 13. Evolution of C-(A)-S-H in the hardened SSC with time.

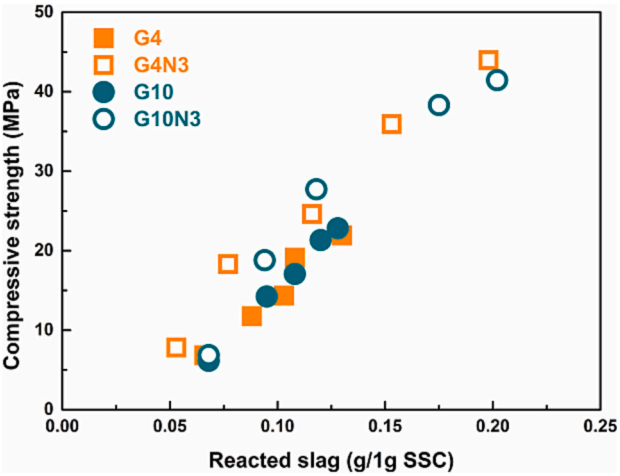

Fig. 14. Compressive strength development of SSC as a function of reacted slag.

4. Discussion

4.1. The factors determining the strength development of SSC

Since slag hydration leads to the formation of C-(A)-S-H and in the presence of gypsum, AFt, then the degree of slag hydration should be closely related to the compressive strength of SSC. It should be noted that the slag contents of the four mixtures (G4, G4N3, G10, G10N3) are slightly different (see Table 2). Thus, while the degree of slag hydration tells us about the reaction kinetics, quantifying the amount of reacted slag could be a more suitable parameter relating to the compressive strength. This is clearly demonstrated in Fig. 14, where a linear correlation could be observed between compressive strength and the amount of reacted slag. However, there is a distinction between the samples without NS (G4 and G10) and with NS (G4N3 and G10N3), but no dependence on gypsum content. For a given quantity of reacted slag, samples containing NS showed slightly higher strengths than those without.

The primary effect of NS on the hardened SSC is its promotion of C-(A)-S-H growth (Fig. 13) and its inhibition of AFt growth (Fig. 11). Thus, use of NS increases the volume ratio of C-(A)-S-H to AFt. It has been found that this ratio is a key factor affecting the compressive strength of sulfoaluminate cements [40]. Through the assumption of the density of C-(A)-S-H (2.48 g/cm^3 [41], some others proposed to be 2.6 g/cm^3 [42], 2.7 g/cm^3 [43]) and AFt (1.78 g/cm^3 [41]), the volume ratio and distribution could be calculated readily. It can be seen from Fig. 15a that addition of NS lowers the AFt/C-(A)-S-H ratio. In addition, the compressive strength of SSC decreases with the ratio of AFt/C-(A)-S-H, as shown in Fig. 15b.

Based on the analysis above, it can be seen that the amount of reacted slag and the volume ratio of AFt/C-(A)-S-H in the hardened SS are two important factors affecting the compressive strength. Therefore, the compressive strength was assumed to be predicted with the formula: $S = A\alpha^n / \beta^m + \gamma$, where α denotes the reacted slag; β denotes the volume ratio of AFt/C-(A)-S-H. Fig. 16 presents the fitting result and the comparison between the measured and predicted compressive strength. The regression coefficient is 0.94, indicating a good fit.

4.2. The role of gypsum in the compressive strength development of SSC

Gypsum is a key component of SSC. Its obvious contribution is in promoting the formation of AFt (Fig. 9). However, higher gypsum contents also increase the degree of slag hydration (Fig. 12), thus increasing the quantity of C-(A)-S-H (Fig. 13). The formation of additional AFt and C-(A)-S-H will affect the volume ratio of AFt/C-(A)-S-H

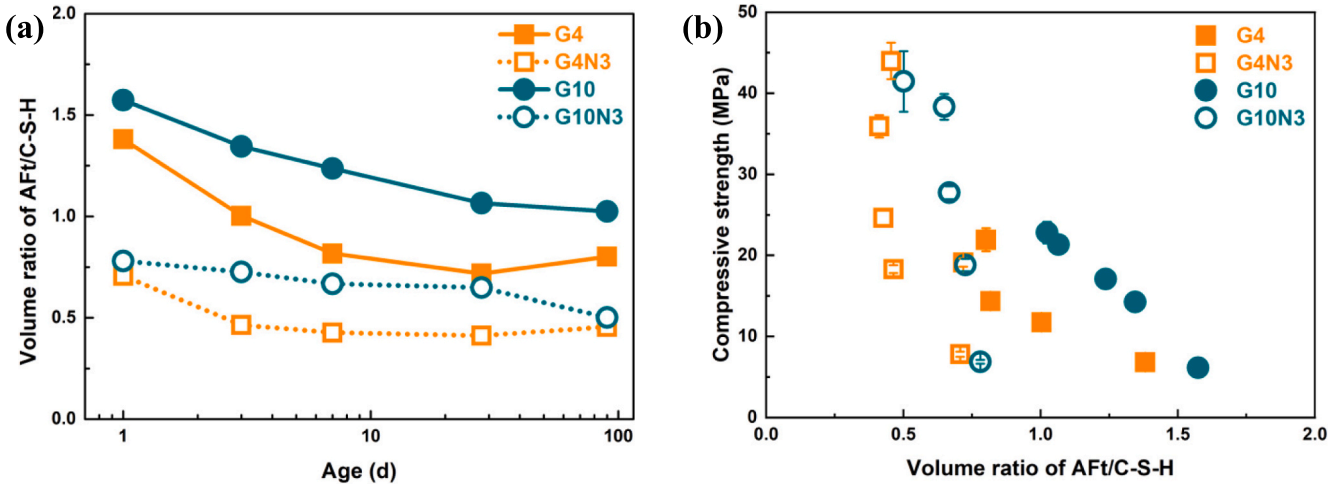

Fig. 15. (a) Volume ratio of AFt/C-(A)-S-H as a function of time and (b) its relation with the compressive strength of SSC.

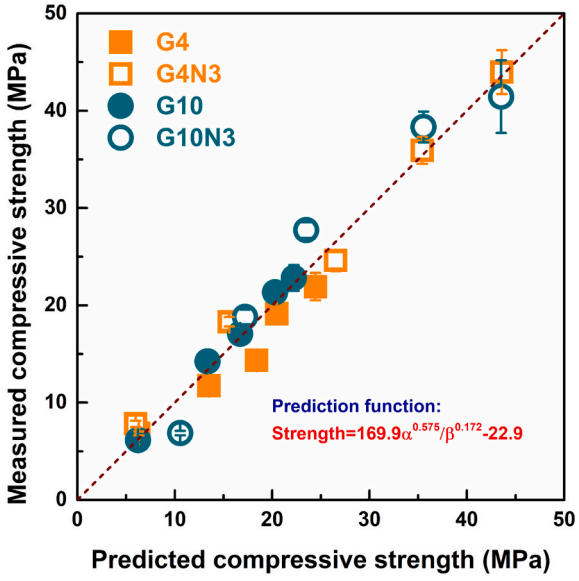

Fig. 16. Comparison between the measured and the predicted compressive strength.

(Fig. 15a). It seems that the enhancing effect of higher gypsum content in accelerating the consumption of slag is partially counteracted by its negative effect through the increase in volume ratio of AFt/C-(A)-S-H.

While not a primary focus of this study, it should be noted that the carbonation resistance of C-S-H is much higher than that of AFt [44]. Therefore, it could be expected that a lower AFt/C-(A)-S-H ratio could improve the carbonation resistance of SSC. So, the gypsum content of SSC could play an important role in the carbonation resistance of SSC, which is part of the ongoing work of the authors.

4.3. The role of NS in the compressive strength development of SSC

There are two other important impacts of NS on the compressive strength of SSC, except the filling effect as found in the Portland cement [33]. One is the reduction in the AFt/C-(A)-S-H volume ratio (see Fig. 15a), and the other is the promotion of slag hydration (see Fig. 12a). Although it has been shown that NS can increase the compressive strength at all ages, different factors are at work at different stages. During the first 7 days, the incorporation of NS inhibits AFt formation (see Fig. 11) and may impede slag hydration when lower gypsum levels are used (see Fig. 12b). However, over time it increases the amount of C-(A)-S-H (see Fig. 13) and reduces the AFt/C-(A)-S-H volume ratio (see Fig. 15a). The higher AFt/C-(A)-S-H volume ratio over the first 7 days is the main reason for the higher compressive strength of samples containing NS. Beyond 7 days, samples containing NS show elevated slag hydration and lower AFt/C-(A)-S-H volume ratios, both of which contribute to the enhancement of compressive strength.

However, what is the reason for the increase in reacted slag by NS? It can be seen from Fig. 12a, b that the degree of slag hydration in the presence of NS increases linearly to 90 days, while in the absence of NS, hydration levels off after 7 days. Thus, something inhibits long-term slag hydration in the systems without NS.

The following several factors are possible reasons. First is the available water for slag hydration. It should be noted that 1 g of AFt contains 0.459 g of water and 1 g of C-S-H ($C_{1.7}SH_2$, as in [24]) contains 0.189 g of water. Therefore, for every gram of AFt not formed, there is sufficient water to form 2.4 g of C-S-H (0.459/0.189 = 2.4). Since in the systems containing NS, the formation of AFt is inhibited (see Fig. 11), and the AFt/C-(A)-S-H volume ratio is reduced (see Fig. 12b), with a fixed amount of mixing water, more hydration products could be formed in the systems containing NS. Second is the available space for hydrate growth. The density of C-(A)-S-H is greater than that of AFt [41], and the addition of NS will increase the degree of polymerization of C-(A)-S-H [45] which will increase the density of C-(A)-S-H further [37,46]. Thus, the lower AFt/C-(A)-S-H volume ratio associated with NS addition will lead to a higher overall density of hydration products, allowing larger available space for more slag hydration at later ages. Third is the distribution of C-(A)-S-H. At hydration proceeds, the diffusion of ions released from slag dissolution could be limiting factors, as in Portland cement systems [47]. It has been shown that the long-term strength of SSC is determined by the formation of C-(A)-S-H [9]. However, diffusion of silicate ions is slow, especially at lower pH [48]. It has been proposed that at lower pH, there exists a layer enriched in Si and Al around the dissolving slag [48]. In this situation, C-(A)-S-H would be precipitated around the slag particles, and the diffusion of free water to the surface of the slag will be slowed. Nevertheless, in the system with NS, the evenly distributed NS will provide many nucleation sites for C-(A)-S-H [38], and promote the precipitation of silicate ions released upon slag dissolution. This would create a silicate sink, preventing the accumulation of an encasing C-(A)-S-H layer around the slag particles. Fourth is the pore solution chemistry of the system, since it provides the driving force of the hydration reaction, however, the thermodynamic and kinetic modelling analysis would be dictated in the author's following contribution.

5. Conclusions

The SSC, containing about 5 % Portland cement, is a classic low-carbon cement. However, its low early-age strength has been one of the factors limiting its practical application. In this study, NS was added into the SSC system, aimed at improving its mechanical properties by promoting the precipitation of C-(A)-S-H. Based on the analysis above, it can be concluded that:

(1) The addition of NS increases the early- (3 days) and late-age (90 days) compressive strength by 35 %–60 % and 80 %–100 %, respectively.
(2) The addition of NS promotes the continuous hydration of slag until the end of the test (90 days), whereas the hydration of slag almost stopped in the absence of NS. This is the main reason for its significant enhancement effect on the compressive strength.
(3) The addition of NS slows down the consumption of gypsum and the formation of AFt, but does not affect their final levels. However, NS does both accelerate the formation of C-(A)-S-H and increase the total amount formed, reducing the AFt/C-(A)-S-H volume ratio and thus providing larger space for the hydration of slag.
(4) The amount of reacted slag (α) and AFt/C-(A)-S-H volume ratio (β) are two important factors dictating the compressive strength (S) of hardened SSC mortars. In this study, their relation may be represented by the formula: $S = 169.9\alpha^{0.58} / \beta^{0.17} - 22.9$.
(5) The gypsum content of SSC only slightly influences the porosity, compressive strength and the hydration of slag; however, higher gypsum content would increase its consumption rate and the total amount of AFt generated, and increase the critical pore radius.

This work proves the significant positive benefits of NS on the performance of SSC by its an asynchronous regulation on the hydration kinetics of silicate and aluminate (promoting the hydration of silicate and inhibiting the hydration of aluminate). It indicated that proper hydration kinetics of silicate and aluminate should be paid more attention in the hydration of SSC and other low-carbon binders with high dosage of SCMs, since both of hydration of silicate and aluminate play a critical role.

CRediT authorship contribution statement

Heng Chen: Conceptualization, Funding acquisition, Methodology, Investigation, Formal analysis, Writing – original draft. **Pengkun Hou:** Conceptualization, Funding acquisition, Resources, Supervision, Writing – review & editing. **Xiangming Zhou:** Writing – review & editing. **Leon Black:** Writing – review & editing. **Samuel Adu-Amankwah:** Writing – review & editing. **Pan Feng:** Writing – review & editing. **Na Cui:** Writing – review & editing. **Michał A. Glinicki:** Writing – review & editing. **Yamei Cai:** Writing – review & editing. **Shipeng Zhang:** Writing – review & editing. **Piqi Zhao:** Supervision, Writing – review & editing. **Qinfei Li:** Supervision, Writing – review & editing. **Xin Cheng:** Funding acquisition, Supervision, Writing – review & editing.

Declaration of competing interest

The authors declare that they have no conflicts of interest.

Data availability

No data was used for the research described in the article.

Acknowledgements

The authors gratefully acknowledge support from National Natural Science Foundation of China (52102021), National Natural Science Foundation of China Regional Innovation and Development Joint Fund (U22A20126), Shandong Province Natural Science Foundation (ZR2021QE058, ZR2020YQ33), Department of Education of Shandong Province (2019GGX102077), Science and Technology Innovation Support Plan for Young Researchers in Institutes of Higher Education in Shandong (2019KJA017). This project has also received funding from the European Union's Horizon 2020 - Research and Innovation Framework Programme under the H2020 Marie Skłodowska-Curie Actions grant agreement No [893469], and funding from Youth Innovation Support Program of Shandong Colleges and Universities, which is also appreciated.

References

[1] M.C.G. Juenger, F. Winnefeld, J.L. Provis, J.H. Ideker, Advances in alternative cementitious binders, Cem. Concr. Res. 41 (2011) 1232–1243.
[2] Q. Wu, Q. Xue, Z. Yu, Research status of super sulfate cement, J. Clean. Prod. 294 (2021), 126228.
[3] R. Masoudi, R.D. Hooton, Influence of alkali lactates on hydration of supersulfated cement, Constr. Build. Mater. 239 (2020), 117844.
[4] S. Liu, J. Ouyang, J. Ren, Mechanism of calcination modification of phosphogypsum and its effect on the hydration properties of phosphogypsum-based supersulfated cement, Constr. Build. Mater. 243 (2020), 118226.
[5] B. Gracioli, C. Angulski da Luz, C.S. Beutler, J.I. Pereira Filho, A. Frare, J.C. Rocha, M. Cheriaf, R.D. Hooton, Influence of the calcination temperature of phosphogypsum on the performance of supersulfated cements, Constr. Build. Mater. 262 (2020), 119961.
[6] F. Winnefeld, B. Lothenbach, Hydration of calcium sulfoaluminate cements — experimental findings and thermodynamic modelling, Cem. Concr. Res. 40 (2010) 1239–1247.
[7] R. Masoudi, R.D. Hooton, Examining the hydration mechanism of supersulfated cements made with high and low-alumina slags, Cem. Concr. Compos. 103 (2019) 193–203.
[8] A. Gruskovnjak, B. Lothenbach, F. Winnefeld, R. Figi, S.C. Ko, M. Adler, U. Mäder, Hydration mechanisms of super sulphated slag cement, Cem. Concr. Res. 38 (2008) 983–992.
[9] T. Matschei, F. Bellmann, J. Stark, Hydration behaviour of sulphate-activated slag cements, Adv. Cem. Res. 17 (2005) 167–178.
[10] I.G. Richardson, A.R. Brough, G.W. Groves, C.M. Dobson, The characterization of hardened alkali-activated blast-furnace slag pastes and the nature of the calcium silicate hydrate (C-S-H) phase, Cem. Concr. Res. 24 (1994) 813–829.
[11] Y. Zhou, Z. Peng, L. Chen, J. Huang, T. Ma, The influence of two types of alkali activators on the microstructure and performance of supersulfated cement concrete: mitigating the strength and carbonation resistance, Cem. Concr. Compos. 118 (2021), 103947.
[12] Y. Briki, M. Zajac, M.B. Haha, K. Scrivener, Factors affecting the reactivity of slag at early and late ages, Cem. Concr. Res. 150 (2021), 106604.
[13] K.L. Scrivener, P. Juilland, P.J.M. Monteiro, Advances in understanding hydration of Portland cement, Cem. Concr. Res. 78 (2015) 38–56.
[14] J.W. Bullard, G.W. Scherer, J.J. Thomas, Time dependent driving forces and the kinetics of tricalcium silicate hydration, Cem. Concr. Res. 74 (2015) 26–34.
[15] G. Land, D. Stephan, The effect of synthesis conditions on the efficiency of C-S-H seeds to accelerate cement hydration, Cem. Concr. Compos. 87 (2018) 73–78.
[16] J. Yu, J. Qian, J. Tang, Z. Ji, Y. Fan, Effect of ettringite seed crystals on the properties of calcium sulphoaluminate cement, Constr. Build. Mater. 207 (2019) 249–257.
[17] X. Liu, P. Hou, H. Chen, Effects of nanosilica on the hydration and hardening properties of slag cement, Constr. Build. Mater. 282 (2021), 122705.
[18] G. Land, D. Stephan, The influence of nano-silica on the hydration of ordinary Portland cement, J. Mater. Sci. 47 (2011) 1011–1017.
[19] B. Ma, J. Mei, H. Li, F. Liu, Influence of nano SiO2 on the hydration and hardening of sulfoaluminate cement (in Chinese), J. Funct. Mater. 47 (2016) 2010–2014.
[20] G. Li, Q. Liu, M. Niu, L. Cao, B. Nan, C. Shi, Characteristic of silica nanoparticles on mechanical performance and microstructure of sulphoaluminate cement/ordinary Portland cement binary blends, Constr. Build. Mater. 242 (2020).
[21] P. Hou, X. Wang, P. Zhao, K. Wang, S. Kawashima, Q. Li, N. Xie, X. Cheng, S. P. Shah, Physicochemical effects of nanosilica on C3A/C3S hydration, J. Am. Ceram. Soc. 103 (2020) 6505–6518.
[22] S. Adu-Amankwah, M. Zajac, C. Stabler, B. Lothenbach, L. Black, Influence of limestone on the hydration of ternary slag cements, Cem. Concr. Res. 100 (2017) 96–109.
[23] K. De Weerdt, K.O. Kjellsen, E. Sellevold, H. Justnes, Synergy between fly ash and limestone powder in ternary cements, Cem. Concr. Compos. 33 (2011) 30–38.
[24] K. Scrivener, R. Snellings, B. Lothenbach, A Practical Guide to Microstructural Analysis of Cementitious Materials, 2015.
[25] B. Li, P. Hou, H. Chen, P. Zhao, P. Du, S. Wang, X. Cheng, GGBS hydration acceleration evidence in supersulfated cement by nanoSiO2, Cem. Concr. Compos. 132 (2022), 104609.
[26] B. Lothenbach, A. Nonat, Calcium silicate hydrates: solid and liquid phase composition, Cem. Concr. Res. 78 (2015) 57–70.

[27] Quantitative Determination of Constituents of Cement, Standards Press of China, Beijing, 2019.
[28] D. Min, T. Mingshu, Formation and expansion of ettringite crystals, Cem. Concr. Res. 24 (1994) 119–126.
[29] C.A.d. Luz, R.D. Hooton, Influence of supersulfated cement composition on hydration process, J. Mater. Civ. Eng. 31 (2019), 04019090.
[30] X. Chen, S. Wu, J. Zhou, Influence of porosity on compressive and tensile strength of cement mortar, Constr. Build. Mater. 40 (2013) 869–874.
[31] G. Li, Properties of high-volume fly ash concrete incorporating nano-SiO2, Cem. Concr. Res. 34 (2004) 1043–1049.
[32] A. P. P, D.K. Nayak, B. Sangoju, R. Kumar, V. Kumar, Effect of nano-silica in concrete: a review, Constr. Build. Mater. 278 (2021), 122347.
[33] A.M. Said, M.S. Zeidan, M.T. Bassuoni, Y. Tian, Properties of concrete incorporating nano-silica, Constr. Build. Mater. 36 (2012) 838–844.
[34] L.P. Singh, S.R. Karade, S.K. Bhattacharyya, M.M. Yousuf, S. Ahalawat, Beneficial role of nanosilica in cement based materials - a review, Constr. Build. Mater. 47 (2013) 1069–1077.
[35] A.M. Cody, H. Lee, R.D. Cody, P.G. Spry, The effects of chemical environment on the nucleation, growth, and stability of ettringite [Ca3Al(OH)6]2(SO4)3·26H2O, Cem. Concr. Res. 34 (2004) 869–881.
[36] F. Pelisser, P.J.P. Gleize, A. Mikowski, Effect of the Ca/Si molar ratio on the micro/nanomechanical properties of synthetic C-S-H measured by nanoindentation, J. Phys. Chem. C 116 (2012) 17219–17227.
[37] W. Kunther, S. Ferreiro, J. Skibsted, Influence of the Ca/Si ratio on the compressive strength of cementitious calcium–silicate–hydrate binders, J. Mater. Chem. A 5 (2017) 17401–17412.
[38] P.K. Hou, S. Kawashima, D.Y. Kong, D.J. Corr, J.S. Qian, S.P. Shah, Modification effects of colloidal nanoSiO(2) on cement hydration and its gel property, Compos. Part B Eng. 45 (2013) 440–448.
[39] F. Sanchez, K. Sobolev, Nanotechnology in concrete – a review, Constr. Build. Mater. 24 (2010) 2060–2071.
[40] J. Li, Study on the Sintering and Hydration Mechanism of a C4A3$-C2S Binary System, 2019 (in Chinese).
[41] B. Lothenbach, D.A. Kulik, T. Matschei, M. Balonis, L. Baquerizo, B. Dilnesa, G. D. Miron, R.J. Myers, Cemdata18: a chemical thermodynamic database for hydrated Portland cements and alkali-activated materials, Cem. Concr. Res. 115 (2019) 472–506.
[42] J.J. Thomas, H.M. Jennings, A.J. Allen, Relationships between composition and density of tobermorite, jennite, and nanoscale CaO−SiO2−H2O, J. Phys. Chem. C 114 (2010) 7594–7601.
[43] A.C.A. Muller, K.L. Scrivener, A.M. Gajewicz, P.J. McDonald, Densification of C-S–H measured by 1H NMR relaxometry, J. Phys. Chem. C 117 (2012) 403–412.
[44] S. Steiner, B. Lothenbach, T. Proske, A. Borgschulte, F. Winnefeld, Effect of relative humidity on the carbonation rate of portlandite, calcium silicate hydrates and ettringite, Cem. Concr. Res. 135 (2020).
[45] M.I.C. Sousa, J.H.d.S. Rêgo, Effect of nanosilica/metakaolin ratio on the calcium alumina silicate hydrate (C-A-S-H) formed in ternary cement pastes, J. Build. Eng. 38 (2021), 102226.
[46] E. Gallucci, X. Zhang, K.L. Scrivener, Effect of temperature on the microstructure of calcium silicate hydrate (C-S-H), Cem. Concr. Res. 53 (2013) 185–195.
[47] J.W. Bullard, H.M. Jennings, R.A. Livingston, A. Nonat, G.W. Scherer, J. S. Schweitzer, K.L. Scrivener, J.J. Thomas, Mechanisms of cement hydration, Cem. Concr. Res. 41 (2011) 1208–1223.
[48] J. Skibsted, R. Snellings, Reactivity of supplementary cementitious materials (SCMs) in cement blends, Cem. Concr. Res. 124 (2019), 105799.